JOURNAL OF CATALYSIS 21, 225–238 (1971)

Kinetics of Bismuth Oxide Reduction with Propylene

F. E. MASSOTH AND D. A. SCARPIELLO

Gulf Research and Development Company, Pittsburgh, Pennsylvania 15230

Received August 21, 1970

Propylene reacts directly with bismuth oxide to give C_6 olefinic products. A kinetic study was undertaken to elucidate the role of the bismuth oxide in this reaction. Experiments were carried out in a flow, microbalance reactor at atmospheric pressure, temperatures from 450 to 550°C and propylene partial pressures of 0.1–1.0 atm, with N_2 as diluent.

Bismuth oxide reduces to bismuth metal in propylene. After extensive reduction, the oxide cannot be completely regenerated due to the melting of the bismuth and consequent collapse of the structure. However, Bi_2O_3 supported on α-Al_2O_3 is regenerable. The rate of reduction increases with temperature and partial pressure of propylene.

Analysis of the results strongly suggests that chemical reaction and bulk diffusion through the product layer are both important in defining the kinetics of the reaction. A model taking into account both processes is used to correlate the data. Since the diffusion rate diminishes with conversion faster than the chemical rate, the initial reduction of the catalyst is mainly limited by surface reaction whereas the continuing reduction is mostly diffusion controlled.

INTRODUCTION

Oxidative dehydrogenation of olefins is currently an active area of catalytic investigation. Most work to date has been carried out with oxygen added to the feed for practical reasons. Catalysis in these systems has been generally explained in terms of a redox-type cycle in which the olefin reacts with the lattice oxygen, followed by immediate reoxidation of the partially depleted catalyst with oxygen from the gas phase (*1*). Such a mechanism is supported, for example, by oxygen-18 exchange studies, which show catalyst lattice oxygen actively participates in the reaction. Catalytic activity is believed to be related to the ease of reduction of the metal cation to a lower valence state. Recently, Batist *et al.* (*2*) have reported extensive studies of the catalytic oxidation of butene over bismuth–molybdate catalysts in the absence of gaseous oxygen. They showed that the nature of the reaction was much the same as that observed during the catalytic reaction in the presence of oxygen.

The previous paper (*3*) has documented the use of bismuth oxide as oxidant for the oxydehydrodimerization of propylene in the absence of gaseous oxygen. Since oxygen from the catalyst is consumed by this reaction, it is necessary to reoxidize the catalyst intermittently. The operation takes on the nature of a batch process with alternate reaction and regeneration cycles. These studies were not able to delineate with certainty the rate-controlling step in the reaction. The object of the present study was to determine the kinetics of the depletive deoxidation of the bismuth oxide with propylene in the absence of oxygen.

Although a myriad of hydrocarbon products are obtained in fixed-bed operation, the primary product using bismuth oxide as oxidant is 1,5-hexadiene. Other products arise from secondary reactions, e.g., isomerization, cyclization, and deep oxidation, of the hexadiene further down

the catalyst bed. By virtue of the flow microbalance technique employed, the kinetic study reported here was confined to the primary step only, i.e., the conversion of propylene to hexadiene.

Theory

For gas–solid reactions of the type,

$$A(\text{gas}) + B(\text{solid}) \rightarrow C(\text{gas}) + D(\text{solid}),$$

after sufficient product has been built up, continuing reaction involves the following consecutive steps:

(1) diffusion of reactant gas A to solid surface D;

(2) adsorption of gas A at exterior surface of solid D;

(3) diffusion of gas A through product layer to solid B-solid D reaction interface;

(4) reaction between A and solid reactant B at reaction interface;

(5) diffusion of product gas C through product layer D to exterior surface;

(6) desorption of product gas C from exterior of solid surface D to gas phase;

(7) diffusion of product gas C to main gas stream.

Although in principle any of these steps could be rate controlling, the domain of gas–solid reaction studies usually encompasses steps (3) and (4). Generally, the complementary steps (1) and (7), (2) and (6), and (3) and (5) are difficult to distinguish experimentally; hence, one only considers steps (1) through (4) as distinct mechanistic processes. Except for engineering situations, where step (1) may represent a real diffusional restriction in large systems, this step is normally not rate limiting. Furthermore, adsorption, step (2), is very rapid at reaction temperatures employed; it is often combined with step (1) and treated as a gas–film transfer resistance. Thus, the problem usually entails differentiation between step (3), bulk diffusion through the product layer, and step (4), chemical reaction at the interface, and characterizing the kinetic parameters of the rate-controlling step. For the reaction of bismuth oxide with propylene at elevated temperature, one of the products is liquid bismuth metal. The presence of a liquid product which adheres to the solid reactant in place of the solid product does not alter the arguments presented.

Phenomenologically, simple diffusion and chemical reaction can be distinguished from the form of the rate equation the experimental data obey, provided data of sufficient accuracy are attainable. Figure 1 pictorially details conceptual differences

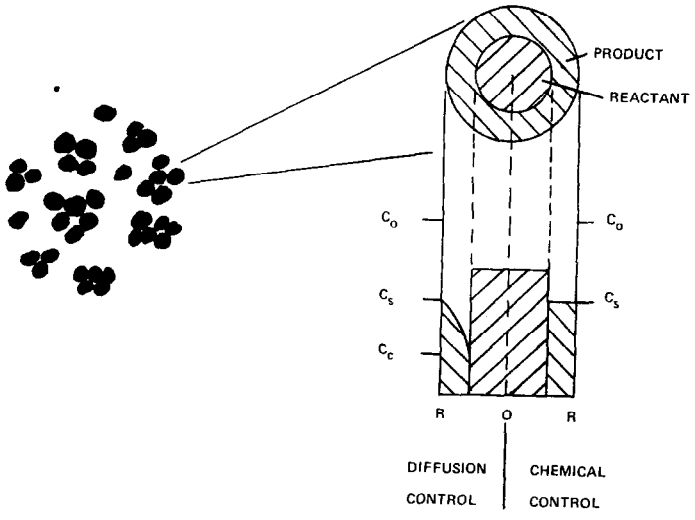

Fig. 1. Reaction model: $A(g) + bB(s) \rightarrow lL(l) + gG(g)$.

between the two mechanisms. The model envisions basic, nonporous particles, which are the centers of reaction. Larger agglomerates of these basic particles make up the powder or larger mesh sizes encountered in actual practice. When reaction at the interface is limiting, the gas concentration remains constant throughout the product layer, whereas in diffusion control, the concentration of diffusing species diminishes from the external surface of the basic particle to the interface.

The integrated rate equation for chemical control takes the form (*4*):

$$k_c t = 1 - (1 - \alpha)^{1/3} = f_c, \qquad (1)$$

where k_c is an apparent surface rate constant, t is time, α is the fraction conversion to product, and f_c represents the function of α shown. This is sometimes called the "contracting sphere model" since it depicts a continually shrinking inner core of reactant material. The rate expression for diffusion through a spherical layer of solid product is given by (*4*):

$$k_d t = 3 - 3(1 - \alpha)^{2/3} - 2\alpha = f_d, \qquad (2)$$

where k_d is an apparent rate constant for diffusion and f_d represents the function of α shown. This form is the spherical cognate of the "parabolic law" commonly encountered in one-dimensional metal oxidations. A plot of f_c or f_d vs time should be linear if either mechanism is operative.

It may occasionally happen that neither the surface reaction nor diffusion are rate limiting, i.e., their relative rates are not too different, or that a change in mechanism from one kinetic controlling regime to another occurs. In this case, which we will show later pertains to the reaction under consideration, both rate processes must be considered in the kinetic evaluation. This can be done by combining the individual rate Eqs. (1) and (2) [Ref. (*5*)] and (see Appendix for derivation), viz.,

$$t = f_c/k_c + f_d/k_d. \qquad (3)$$

Hence, a test for data fit in this case takes on the form,

$$t/f_c = 1/k_c + (1/k_d)(f_d/f_c), \qquad (4)$$

where (t/f_c) is plotted against (f_d/f_c).

Effect of Temperature and Pressure on Reaction Rates

We have described the reduction of Bi_2O_3 with propylene in terms of two rate constants, k_c, representing chemical reaction at the metal–metal oxide interface and k_d, representing diffusion of a reactive species through the melted bismuth product layer covering the oxide. Since both are activated processes, an Arrhenius-type dependency of rate constant with temperature would be expected, viz.,

$$k = A \exp(-E_a/R_g T), \qquad (5)$$

where A is the preexponential factor, E_a the apparent activation energy, R_g the gas constant, and T the absolute temperature. Although the relationship is general in nature, the significance of the activation energy is dependent upon the assumed mechanism.

The incorporation of pressure into the reaction rate constants for gas–solid reactions is more complex—a generalized expression cannot be written as with temperature. Thus, a mechanism must be assumed and compared to the experimental data. It is common to assume first order in reactant gas pressure for simplicity, although many cases of fractional order and even changing order of pressure dependence during reaction have been observed.

Since the limiting reaction sequence envisaged for the reduction of Bi_2O_3 with propylene involves diffusion of a reactive species through a molten Bi layer followed by reaction at the oxide surface, an increase in propylene pressure should increase the diffusing species and availability of active material at the reaction interface. Since the solubility of propylene in molten bismuth would be expected to be low, Henry's law should be valid. Thus,

$$C_s = Hp, \qquad (6)$$

where C_s is the concentration of propylene in the molten bismuth at the external surface of the basic particle, p is the propylene

partial pressure in the gas phase, and H is the coefficient of solubility. Recalling the combined kinetic expression, Eq. (3), the rate constants are related to the basic parameters by (see Appendix);

$$k_c = bMk_iC_s/R\rho \quad (7)$$

and

$$k_d = 6bMDC_s/R^2\rho, \quad (8)$$

where b is the number of moles of Bi_2O_3 reacting per mole of propylene; M is the molecular weight of Bi_2O_3; k_i is the chemical rate constant at the Bi–Bi_2O_3 interface; ρ is the density of Bi_2O_3; R is the basic particle radius; D is the diffusion coefficient. Inserting Eq. (6) into (7) and (8) yields,

$$k_c = bMk_iHp/R\rho = B_cp \quad (9)$$

and

$$k_d = 6bMDHp/R^2\rho = B_dp. \quad (10)$$

Thus, the experimentally derived rate constants k_c and k_d should be directly proportional to the propylene pressure.

Experimental

Unsupported bismuth oxide was prepared by calcination of reagent grade $Bi(NO_3)_3 \cdot 5H_2O$ at 600°C. The sample was ground and screened to −325 mesh. Surface area of the oxide determined by krypton adsorption was 1.5 m^2/g, corresponding to an average basic particle size of 0.45 μ. Particle sieve analysis showed the average size to be about 1 μ. Photomicrographs taken at magnifications of 625 and 2500 clearly show clusters of aggregates made up of many smaller, approximately spherical particles of the order of 0.1–1 μ in size. This picture agrees well with surface area and sieve measurements. Therefore, the powdered bismuth oxide catalyst consists of aggregates of loosely held, nonporous basic particles. The basic material, according to X-ray analysis, was mainly α-Bi_2O_3, with a minor amount of γ-Bi_2O_3.

Supported bismuth oxide was prepared by impregnation of α-alumina with a bismuth nitrate solution. The incipient-wetted material was evaporated to dryness, followed by calcination at 550°C for 16 hr. Analysis gave 25.9 wt% Bi_2O_3.

In heating in air to reaction temperature (500°C), the sample lost 2.6% weight, the loss commencing at about 425°C. The nitrogen content of the charge was less than 0.003 wt% by analysis, precluding the source of the weight loss as due to residual nitrate. Thermal gravimetric analysis of $Bi(NO_3)_3 \cdot 5H_2O$ confirmed that complete decomposition to Bi_2O_3 occurs above 560°C. We attribute the loss to water adsorbed on the oxide during exposure of the sample to the atmosphere at room temperature.

A pretreatment period was established so that the thermal history of each sample was the same. This consisted of subjecting the Bi_2O_3 to an air atmosphere treatment at 500°C for either 2 hr or overnight (16 hr).

The propylene used was technical grade of 97% purity. Nitrogen was used to dilute the hydrocarbon to the desired partial pressure. The nitrogen was purified by passing it over hot copper turnings to remove oxygen followed by type 4A molecular sieves for drying. Ultrahigh-purity hydrogen was passed through a deoxo unit before drying with molecular sieves. Various partial pressures of mixtures were achieved by flow metering individual streams.

A Cahn microbalance was used in a flow system at atmospheric pressure to provide a continuous record of weight change with time. A sample of approximately 300 mg was charged in a quartz bucket suspended by a series of quartz rods from the balance arm. Weight changes were read to the nearest 0.05 mg. The assembly was enclosed in a quartz-tube reactor which was heated by a conventional furnace. Temperature control was within ±2°C of the desired temperature. Gas rates employed were 400 cm^3/min total flow. Quartz chips were located at the bottom of the reactor tube (inlet) to preheat the incoming gas stream. Small buoyancy corrections were applied to the weight changes by reference to a standard nitrogen flow before and after reaction.

The isothermal character of the reduction was checked by using another reactor assembly of similar geometry and identical flow conditions to that employed in the kinetic studies. A microthermocouple was placed in the sample contained in the bucket and the temperature rise attending reaction was monitored. Reduction of the bismuth oxide in a hydrogen partial pressure of 0.1 atm at 500°C gave a temperature rise above ambient sample temperature of only 4°C, followed by a gradual decay to reactor temperature. Hydrogen was employed instead of propylene for convenience. Since the rate of reduction in hydrogen was appreciably faster than in propylene, it can be safely concluded that the propylene runs were essentially isothermal.

Vaporization of liquid bismuth (mp = 271°C) is negligible at reaction temperatures employed (*6*), as is that of the oxide (mp = 820°C). Gas chromatographic analysis of reaction products from the microbalance reactor was achieved employing a 50 ft × ¼ in. column packed with Dow-Corning 200 silicone. Flame ionization detection was used because of the low concentrations of C_6-products (<500 ppm). Consequently, carbon oxides could not be measured in this analysis.

Results

Preliminary Runs

A thermogravimetric analysis of the reduction of Bi_2O_3 in H_2 showed that no appreciable reaction occurred up to a temperature of 260°C. Above this temperature, the reduction rate increased rapidly and reduction to elemental Bi was complete at 500°C. The sample did not reoxidize at this temperature upon treatment with air. Examination revealed the presence of globules of metal fused to the quartz bucket. This is not unexpected, since the reaction temperature is well above the melting point of bismuth metal.

Propylene reduction of Bi_2O_3 was studied at 500°C. Nitrogen was added to the propylene flow so that the partial pressure of propylene was 0.22 atm. The propylene-N_2 flow was continued overnight. A high degree of reduction to elemental bismuth (93%) was obtained. On reoxidation for a weekend period, weight gain accounted for 63% of total conversion back to bismuth oxide. Visual inspection of the sample showed the presence of metallic Bi particles interspersed among the oxide particles. We conclude that propylene can reduce the Bi_2O_3 to Bi metal, but that complete regeneration of the Bi_2O_3 is not possible after a high degree of reduction.

Several runs were made to test for reproducibility. Results are shown in Fig. 2, where conversion to Bi metal, α, is plotted against time. Duplicate runs on the same batch of Bi_2O_3 checked within 10%. Decreasing the sample size by a factor of three had no effect on the rate of conversion, indicating that gas-diffusional effects are nil. The addition of 0.6 or 3.0 mole % H_2O vapor had no effect on reduction rates, showing the absence of product H_2O inhibition.

It should be noted that the α-plot of Fig. 2 shows no break in curvature, signifying the absence of any appreciable intermediate oxides of bismuth, notably Bi_2O_2. X-Ray diffraction analysis confirmed the presence of only Bi and unreacted Bi_2O_3.

To evaluate the influence of bulk particle diffusion on the reaction kinetics, another batch of relatively large particles, 10–20 mesh, was secured, a portion of this being ground to a fine powder. Both the large particles and ground material had identical surface areas of 0.5 m^2/g by krypton measurement. The fact that reducing the gross particle size had no effect on the surface area is in accord with the particle morphology pictured above; viz., the large particles are made of loosely held aggregates of basic particles, with complete internal accessibility of gas to the basic particles. Both the 10–20 mesh particles and the ground material reacted with propylene at an identical rate. Hence, the absence of gas-diffusional effects is verified. It should also be mentioned that the

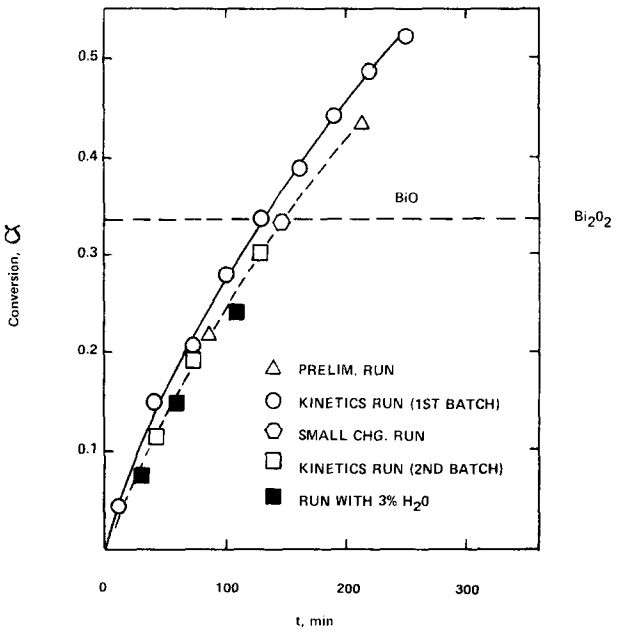

FIG. 2. Reduction of Bi_2O_3 in propylene, where T = 500°C; P = 1 atm, and pC_3H_6 = 0.22 atm.

overall rate of reaction was slower than for the original —325 mesh powder under identical reaction conditions, which is qualitatively in accord with our reaction model. Thus, the 10–20 mesh batch, having a lower surface area, contains larger basic particles on the average than the —325 mesh powder, and consequently will have a lower rate of conversion.

In order to establish the nature of the products formed during reaction in the microbalance, the reactor effluent was analyzed by gas chromatography for hydrocarbons, the results of which are given in Fig. 3. The major product found was 1,5-hexadiene, with lesser amounts of 1,3-hexadiene and benzene. Peak 3 is assigned to 1,4-hexadiene and peak 5 to 1,3-cyclohexadiene. The mole ratio of hexadienes to other C_6-products is estimated to be 15 to 1. In order to check the extent of thermal decomposition of propylene, a repeat run was made under the same conditions, using quartz chips in place of the bismuth oxide. The dotted line shows the resultant chromatogram obtained. Evidently, the two shoulders on the 1,5-hexadiene peak are due to thermal cracking of propylene. Carbon oxides could not be analyzed by the method used; however, their presence would be expected to be extremely small based on selectivity data from fixed-bed runs under similar conditions (*3*). Overall, we conclude that the major reaction occurring between bismuth oxide and propylene in the microbalance reactor is formation of hexadienes,

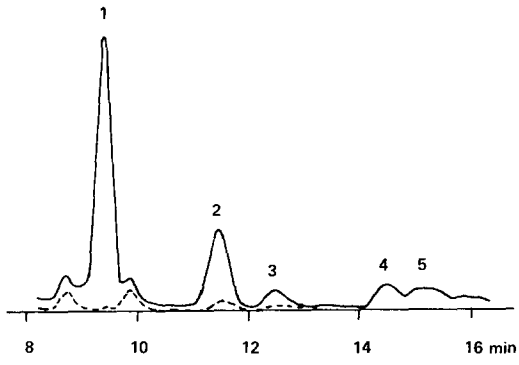

FIG. 3. Analysis of hydrocarbon products from microbalance reactor, with pC_3H_6 = 0.5 atm; T = 500°C; α = 0.035.

Peak 1, 1,5-hexadiene; peak 2, 1,3-hexadiene; peak 3, 1,4-hexadiene; peak 4, benzene; and peak 5, 1,3-cyclohexadiene.

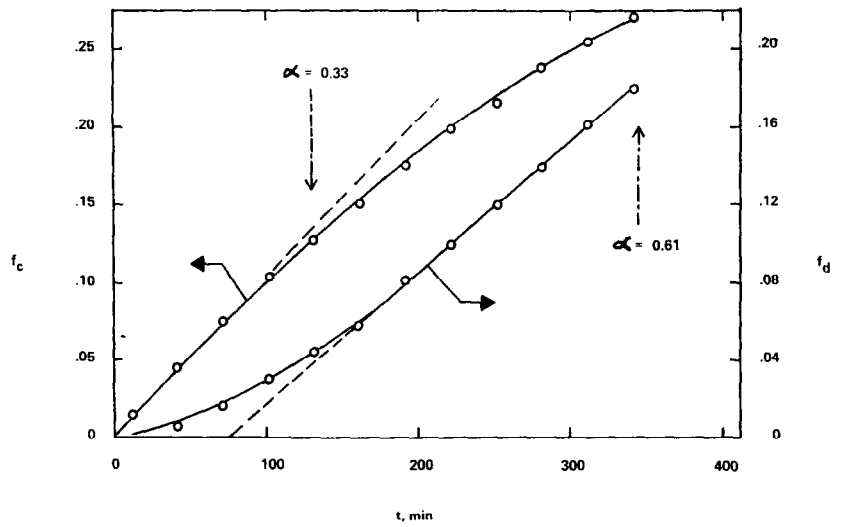

FIG. 4. Chemical vs diffusion control correlation, where T = 500°C and pC_3H_6 = 0.22 atm.

with secondary reaction to further dehydrogenated products of minor importance.

Kinetic Runs

An example of the data obtained for the kinetic analyses is shown in Fig. 2 (open circles); values of conversion, α, are calculated from the continuous microbalance recording of weight loss with time and weight of Bi_2O_3 in the sample. Reaction rate continuously diminished with increasing conversion. In order to test whether the reaction is surface-controlled or diffusion-controlled, the data were replotted according to Eqs. (1) and (2), respectively. The resultant fits are illustrated in Fig. 4, where curvature from the predicted straight lines is observed. Neither mechanism alone appears to adequately fit all the data; the results suggest conformance to surface-reaction control in the early stages of reaction and to diffusion control in the later stages. The surface reaction appears to be limiting in the first third of the reduction.

In order to test the hypothesis of changing reaction control with conversion, resort was made to Eq. (4) for combined rate-controlling steps. Figure 5 shows this fit. From the slope and intercept values, individual rate constants were calculated to be: $k_c = 1.25 \times 10^{-3}$ min^{-1} and $k_d = 1.50 \times 10^{-3}$ min^{-1}. The proximity of the two constants attests to the fact that neither rate step is controlling. The integrated rate equation from the above combined rate analysis is:

$$t = 8.0 \times 10^2[1 - (1 - \alpha)^{1/3}] + 6.7 \times 10^2[3 - 3(1 - \alpha)^{2/3} - 2\alpha], \quad (14)$$

where t is in min, and α is the fraction conversion of Bi_2O_3 to Bi. The closeness of fit of this expression to the experimental data is shown by the solid line passing through the open circle points in Fig. 2.

Figure 6 illustrates the influence of temperature and propylene partial pressure on the course of the reduction of Bi_2O_3.* Increasing temperature and partial pressure caused an increase in the overall conversion to Bi, as expected. These data were treated using the combined kinetic expression, Eq. (4), to obtain values of the chemical rate constants and the diffusion rate constants by least squares analysis.

Variation of the derived rate constants with temperature is depicted in Fig. 7. The satisfactory straight lines obtained confirm

* The two sets of data are not internally consistent since a different batch of oxide was employed for each set, that for the pressure series having a slightly lower reactivity (see Fig. 2).

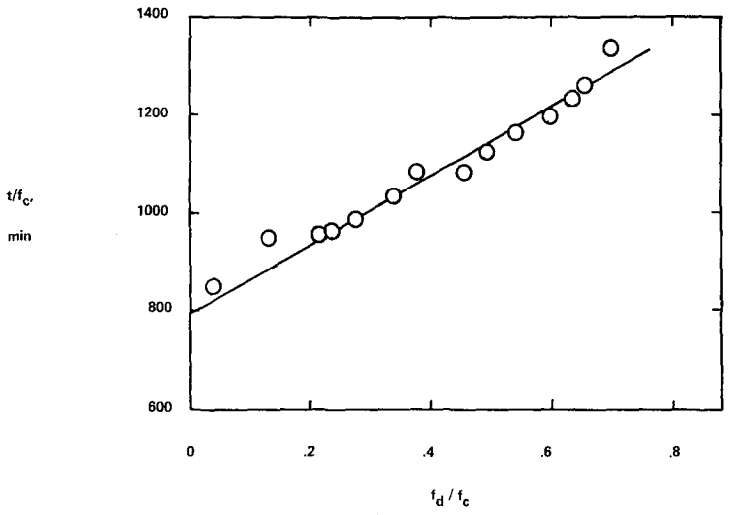

FIG. 5. Combined chemical and diffusion control, where T = 500°C and pC_3H_6 = 0.22 atm.

that Arrhenius-type relationships are obeyed by both rate steps. The experimental activation energies derived from least square analyses of the plots are 27 kcal/mole for the chemical reaction and 20 kcal/mole for the diffusion process. The former value is in the range for chemical reactions, especially for metal oxide reductions. The latter value is also reasonable if it is remembered that the diffusion process represents an activated, volume diffusion of a dissolved species through a molten metal layer and not gas diffusion through a porous layer, as is normally encountered in porous catalysts.

The influence of propylene pressure on the rate constants is shown in Fig. 8. The first-order dependency predicted by the proposed model (see Theory) is obeyed for both rate constants. The partial pressure plots show more variance in the diffusion rate constants than the chemical rate con-

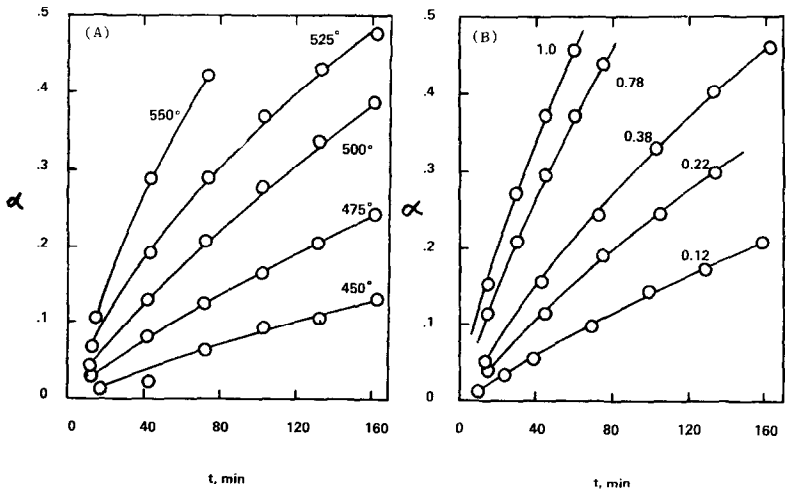

FIG. 6. Temperature effect: pC_3H_6 = 0.22 atm and the Nos. refer to temp., °C. Pressure effect: T = 500°C and the Nos. refer to pC_3H_6 atm.

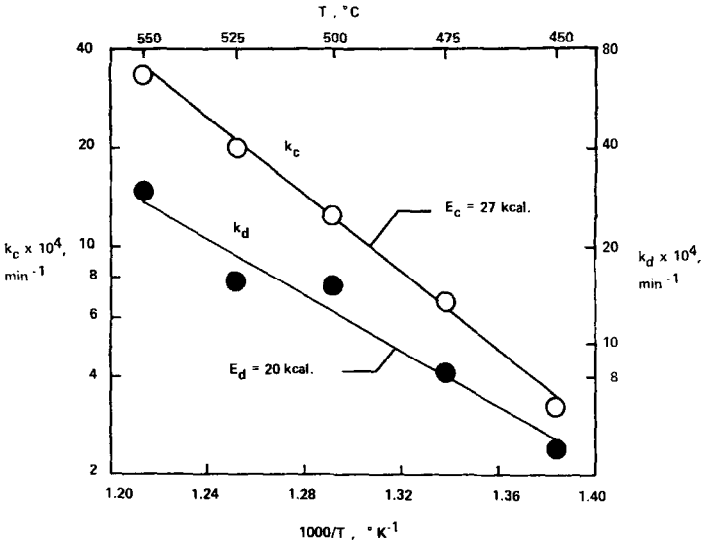

FIG. 7. Variation of rate constants with temperature, where pC_3H_6 = 0.22 atm, T, °C.

stants, which is also observed for the temperature plots, Fig. 7. The larger deviation is probably due to the fact that some of the runs were not continued for a long enough time to obtain sufficient data in the diffusion regime.

At low propylene pressures an induction period was noted. Figure 9 shows the gen-

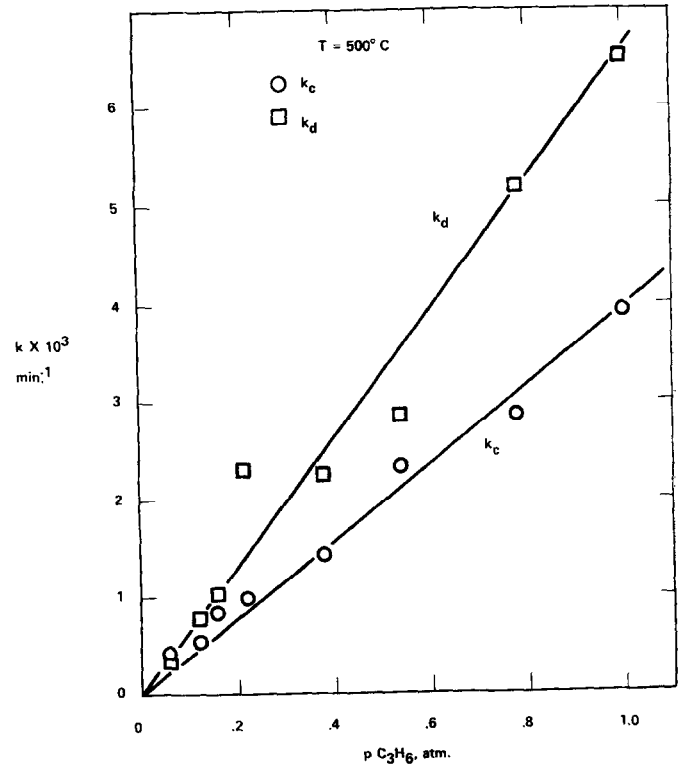

FIG. 8. Variation of rate constants with propylene partial pressure.

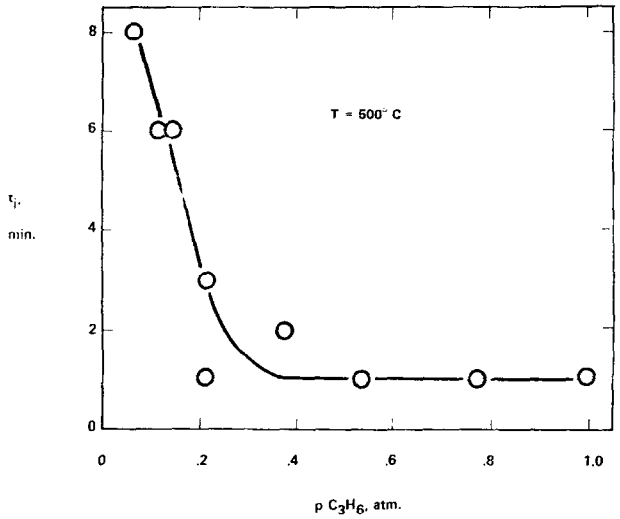

FIG. 9. Variation in induction time with propylene pressure.

eral trend of the measured induction times with partial pressure. No induction was observed for propylene pressures above 0.2 atm; the 1-min base line is due to apparatus hold-up time. However, at low pressure an appreciable time is required before reaction commences. Induction periods are common in many oxide reductions, e.g., MnO_2 (*7*), CoO (*8*), and NiO (*9, 10*), being generally ascribed to slow growth of surface nuclei. Long induction times are usually prevalent at low pressures and low temperatures.

The reaction of propylene with supported Bi_2O_3 was only briefly investigated. The course of the reduction was similar for this material as the bulk Bi_2O_3, i.e., both chemical and diffusion steps were important to the kinetic analysis. Rate constants derived from the combined analysis for reaction at 500°C and 0.22 atm partial pressure of propylene were: $k_c = 3.2 \times 10^{-3}$ min^{-1} and $k_d = 13.7 \times 10^{-3}$ min^{-1}. These are to be compared to average values of 1.25×10^{-3} and 1.50×10^{-3}, respectively, for the bulk material. Assuming the support has no effect on reduction, we estimate the specific surface area of the Bi_2O_3 on the support to be about three times the bulk.*

* From Eq. (7), $R_{bulk}/R_{support} = k_{c,support}/k_{c,bulk} = 2.6$. Alternatively, from Eq. (8), $R_{bulk}/R_{support} = \sqrt{k_{d,support}/k_{d,bulk}} = 2.9$. The specific areas are reciprocally related to the radii.

Regeneration

Depending on the degree of reduction, reoxidation of the bulk oxide back to Bi_2O_3 may or may not be complete. Figure 10 relates the degree of reoxidation in air at 500°C with extent of prior reduction. When the sample was less than 60% reduced, complete reoxidation was achieved; if more than 60% reduced, reoxidation fell off with the degree of reduction. X-Ray examination of a completely reoxidized sample revealed only α-Bi_2O_3. The incompletely oxidized sample which had been completely reduced, showed in postvisual inspection, the presence of bismuth metal particles

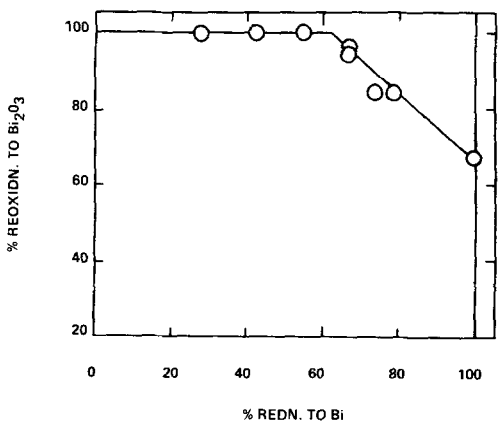

FIG. 10. Catalyst regeneration.

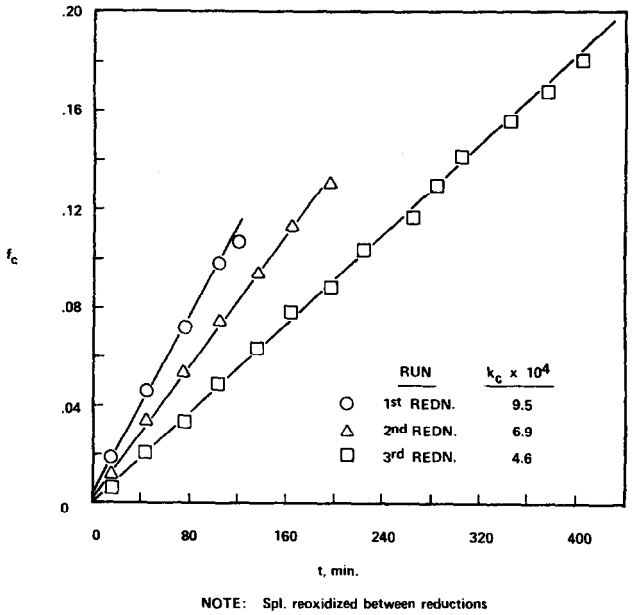

FIG. 11. Reoxidation effect on subsequent reduction — chemical step with T 500°C.

interspersed among oxide particles. X-Ray analysis detected only phases attributable to Bi and α-Bi_2O_3.

In order to assess whether completely reoxidized samples are restored to their initial reactivity, repeat reduction–oxidation cycles were performed. Figure 11 shows that catalyst chemical reactivity towards reduction was lower for the second and third reduction cycles.

Regeneration of the reduced supported bismuth oxide was appreciably better than for the bulk. For example, after 95% reduction of the supported bismuth oxide, 92% reoxidation was achieved upon regeneration. Nevertheless, subsequent reduction rates after regeneration were again lower than for the original catalyst, the effect, however, being not as marked. After 10 reaction–regeneration cycles, the value of k_c had decreased from 3.2 to 1.3×10^{-3} min^{-1}, and k_d from 13.7 to 1.82×10^{-3} min^{-1}. That the reaction mechanism had not essentially changed due to repeated regenerations is evidenced by the k_c and k_d ratios fresh and after the ten regeneration cycles, *viz.*, $k_c^f/k_c^a = 2.5$ and $(k_d^f/k_d^a)^{1/2} = 2.7$, it being recalled that $k_c \propto 1/R$ while $k_d^{1/2} \propto 1/R$. Consequently, only the total bismuth oxide area had been affected by regeneration.

DISCUSSION

The flow microbalance reactor is a convenient technique for studying kinetics of gas–solid reactions involving single-step reactions since weight changes are directly monitored. The method suffers in complex cases when very fast secondary reactions occur between gas products and solid reactant, owing to the ambiguity of ascribing weight changes to more than one reaction. In the latter case, one must supplement the balance results with gas product analyses. However, the geometric configuration of the microbalance reactor, which uses a small amount of solid and large relative gas flows, tends to minimize secondary reactions.

In the present study, our kinetic analysis pertains to the removal of lattice oxygen by reaction with propylene to form hexadienes. Gas product analysis confirmed that this was the major reaction occurring in the microbalance reactor. The low concentration of hexadienes produced relative to

propylene reactant concentration assures that secondary reactions which consume oxygen are minimal. Obviously, if appreciable amounts of dehydrogenated products were obtained, e.g., cyclohexadiene, benzene, or carbon oxides, the kinetic analysis would have been complicated because of the removal of more than one oxide atom per mole of product.

The results obtained in the present investigation suggest that the reduction of bismuth oxide with propylene proceeds through two discernible mechanism steps, viz, chemical surface reaction and bulk diffusion through the product layer. That both steps are detectable by kinetic analysis is derived from the fact that both rates are of similar order of magnitude. The basic nature of the change in rate with degree of reduction then dictates that chemical reaction should prevail in the early stages of reaction while diffusion should dominate in the later stages. Examples of other reactions in which both chemical reaction and diffusion were found to be kinetically important are: reaction of silver with sulfur vapor (*5*) and reduction of iron sulfide with hydrogen (*11*). The data fit our model up to at least 0.8 conversion, after which they deviate from prediction. The model kinetics apply strictly to material of uniform particle size. When a distribution of particle sizes exists, as is normal for most samples, deviations from the kinetic expressions will occur, being most pronounced near the end of the reaction. However, to determine the significant reaction steps and activation energy, it is only necessary that the sample be identical in all runs with respect to size distribution and particle shape (*12*). Our experimentally determined activation energies are reasonable, and first order dependence in propylene is generally obeyed, as predicted.

Concerning reoxidation of the partially reduced catalyst, it is most reasonable to ascribe the lack of complete reoxidation when reduction has proceeded too far, to sintering of the basic catalyst particles. Earlier work had shown a fresh catalyst having a surface area of 1.5 m^2/g had undergone a diminution in area to 0.2 m^2/g after repeated reduction-oxidation cycles in fixed-bed operation (*3*). This is easy to understand when it is recalled that the bismuth layer formed around the remaining oxide core is liquid at reaction temperatures studied. Normal contact between the basic particles in an agglomerate will cause a certain amount of 'necking' between the particles, with eventual growth of the neck area and consequent fusing of the particles. This phenomenom will be all the more pronounced with the degree of reduction since there is an overall molar volume contraction of about 20% in going from oxide to bismuth metal. The surface area demise due to reduction is undoubtedly the cause for the lower reduction rates obtained on second and third cycle reductions (Fig. 11), even though reoxidation was completely achieved after each partial reduction step. A catalytic manifestation of this sintering process is a decrease in activity for propylene conversion observed with several reduction–oxidation cycles.

On the other hand, the supported bismuth oxide catalyst shows excellent regeneration characteristics, complete reoxidation to the original oxide state being achieved even after a high degree of reduction. We believe this is due to the influence of the support structure; the bismuth oxide particles, being dispersed within the pores of the support, are physically prevented from appreciable contact with each other. Upon reduction, only those localized particles within the same pore have the opportunity of sintering, the support matrix preventing massive coalescence. Thus, only partial sintering will occur, which, however, is not of sufficient magnitude to prevent total reoxidation. Nevertheless, this limited sintering is manifested in lower reduction rates with recycle, although in this case, the effect is much less marked than for the bulk bismuth oxide.

Conclusions

The present investigation supports the following conclusions:

(1) Bulk bismuth oxide consists of aggregates of loosely held, nonporous particles of micron size.
(2) Bi_2O_3 reduces in propylene to Bi metal without going through any stable intermediate states.
(3) The kinetics of the reduction are satisfactorily described by a model invoking an initial chemical-controlled reaction followed by a later diffusion-limited regime.
(4) Reduction rates of oxide to bismuth metal in propylene increase with temperature and pressure, but are unaffected by water vapor or gross particle size up to at least 10–20 mesh, provided the same basic particle size is present.
(5) Apparent activation energies for the chemical and diffusion steps are 27 and 20 kcal/mole, respectively.
(6) Chemical and diffusion rates are first-order in propylene partial pressure.
(7) An induction period is observed at low propylene pressure.
(8) Sintering of the bulk oxide occurs during reduction, and
(9) Complete reoxidation of the bulk oxide is not possible beyond 60% reduction; the supported bismuth oxide is completely regenerable.

Appendix

In deriving a basic equation expressing the kinetics of the reduction of bismuth oxide with propylene the following assumptions are made:

(1) Only chemical reaction at the oxide–metal interface and diffusion through the liquid metal product layer are rate controlling;

(2) Complete and instantaneous accessibility of propylene to all basic particles of oxide;

(3) The basic particles are spherical in shape and uniform in size.

(4) At any given time, steady-state diffusion can be safely invoked.

(5) Overall particle size does not change during reaction.

(6) The mean diffusivities of gaseous reactants and products through the liquid metal layer are equal.

The state of a partially reacted particle is shown in the following diagram. The

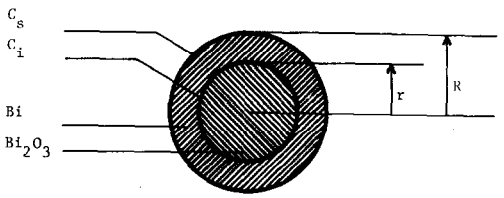

center core of unreacted oxide having a radius r, is surrounded by an outer layer of liquid metal, the overall particle radius being designated as R. The rate of diffusion of gas through a spherical shell is given by Barrer (*13*) as,

$$\frac{dN}{dt} = \frac{4\pi Rr}{R - r} D(C_s - C_i), \qquad \text{(A-1)}$$

where N is the diffusion flux, t is time, D is the diffusivity of the diffusing species and C_s and C_i are the reactant gas concentrations at the outer surface and reaction interface, respectively. The chemical reaction at the interface is given by,

$$\frac{dN}{dt} = 4\pi r^2 k_i C_i, \qquad \text{(A-2)}$$

where k_i is the intrinsic surface reaction rate constant. The rate of consumption of oxide is

$$\frac{dN_{ox}}{dt} = \frac{1}{b}\frac{dN}{dt} = -\frac{4\pi r^2 \rho}{bM}\frac{dr}{dt}, \qquad \text{(A-3)}$$

where b is the stoichiometric number of moles of oxide reacting per mole of gas reactant, and ρ and M are the density and molecular weight of the oxide, respectively. Finally, from the geometry of the reacting particle,

$$\alpha = 1 - (r/R)^3, \qquad \text{(A-4)}$$

where α is the fraction of oxide converted to metal. Equations (A-1) to (A-4), together with appropriate boundary conditions, are sufficient to derive an explicit ex-

pression for fraction converted in terms of reaction time and system parameters.

We proceed by equating (A-1) and (A-2) and solving for C_i, which gives,

$$C_i = \frac{C_s}{1 + (1 - r/R)(r/R)k_iR/D}. \quad \text{(A-5)}$$

Inserting (A-5) into (A-2) and combining with (A-3) yields,

$$\frac{d(r/R)}{dt} = -\frac{k_ibMC_s}{\rho R} \times \frac{1}{1 + (1 - r/R)(r/R)k_iR/D}. \quad \text{(A-6)}$$

This differential equation is to be solved subject to the following boundary conditions:

$$\begin{aligned} t &= 0,\ r/R = 1 \\ t &= t,\ r/R = r/R. \end{aligned} \quad \text{(A-7)}$$

The solution of (A-6) and (A-7) leads to,

$$\frac{bMC_st}{\rho R} = \frac{1}{k_i}(1 - r/R) + \frac{R}{6D} \times \{3[1 - (r/R)^2] - 2[1 - (r/R)^3]\} \quad \text{(A-8)}$$

Now, let

$$\begin{aligned} k_s &= bMk_i\,C_s/\rho R \\ k_d &= 6bMDC_s/\rho R^2 \end{aligned} \quad \text{(A-9)}$$

Insertion of (A-9) into (A-8) and incorporation of (A-4) leads to:

$$t = \frac{1}{k_c}[1 - (1 - \alpha)^{1/3}] + \frac{1}{k_d}[3 - 3(1 - \alpha)^{2/3} - 2\alpha] \quad \text{(A-10)}$$

or,

$$t = \frac{f_c}{k_c} + \frac{f_d}{k_d} \quad \text{(A-11)}$$

where:

$$\begin{aligned} f_c &= 1 - (1 - \alpha)^{1/3} \\ f_d &= 3 - 3(1 - \alpha)^{2/3} - 2\alpha \end{aligned}$$

which is our desired kinetic expression equivalent to equation (3) in the text.

It should be noted that k_c and k_d contain the surface concentration, C_s, which is generally unknown. If C_s can be expressed in terms of an adsorption isotherm (for solids) or a solubility relationship (for liquids), the respective rate constants can be related to the system pressure as is demonstrated in the Theory section.

Acknowledgments

The authors wish to thank Mr. W. E. Faust for assistance with the experimental work and Mrs. W. R. Larson for the X-ray analyses.

References

1. Cullis, C. F., *Ind. Eng. Chem.* **59** (12), 18 (1967).
2. Batist, Ph.A., Kapteijns, C. J., Lippens, B. C., and Schuit, G. C. A., *J. Catal.* **7**, 33 (1967).
3. Swift, H. E., Bozik, J. E., and Ondrey, J. A., *J. Catal.* **21**, 212 (1971).
4. Levenspiel, O., "Chemical Reaction Engineering." Chap. 12. Wiley, New York, 1962.
5. Billy, M., and Valensi, G., *J. Chim. Phys. Physicochim. Biol.* **1956**, 832 (1956).
6. Nesmeyanov, A. N., "Vapor Pressure of the Chemical Elements." Elsevier Publ. Co., 1963.
7. Barner, H. E., and Mantell, C. L., *Ind. Eng. Chem. Process Des. Develop.* **7**, 285 (1968).
8. Verhoeven, W., and Delmon, B., *Bull. Soc. Chim. Fr.* **1966**, 3065 (1966).
9. Delmon, B., *Bull. Soc. Chim. Fr.* **1961**, 590 (1961).
10. Benton, A., and Emmett, P., *J. Amer. Chem. Soc.* **46**, 2728 (1924).
11. Shien, J., and Smith, J. M., *Ind. Eng. Chem. Fundam.* **4**, 293 (1965).
12. Carter, R., *J. Chem. Phys.* **34**, 2010 (1961).
13. Barrer, M., *Phil. Mag.* **35**, 802 (1944).